Mon. Not. R. Astron. Soc. **000**, 1–16 (2011) Printed 10 October 2014 (MN LATEX style file v2.2)

# The state of globular clusters at birth II: primordial binaries

Nathan Leigh[1,2], Mirek Giersz[3], Michael Marks[4], Jeremy J. Webb[5], Arkadiusz Hypki[3,6], Craig Heinke[1], Pavel Kroupa[4], Alison Sills[5] ⋆

[1] *Department of Physics, University of Alberta, CCIS 4-183, Edmonton, AB T6G 2E1, Canada*
[2] *Department of Astrophysics, American Museum of Natural History, Central Park West and 79th Street, New York, NY 10024*
[3] *Nicolaus Copernicus Astronomical Centre, Polish Academy of Sciences, ul. Bartycka 18, 00-716 Warsaw, Poland*
[4] *Helmholtz-Institut für Strahlen- und Kernphysik, Nussallee 14-16, D-53115, Bonn, Germany*
[5] *McMaster University, Department of Physics and Astronomy, 1280 Main St. W., Hamilton, Ontario, Canada, L8S 4M1*
[6] *Leiden Observatory, Leiden University, P.O. Box 9513, 2300 RA Leiden, The Netherlands*

arXiv:1410.2248v1 [astro-ph.SR] 8 Oct 2014

10 October 2014

**ABSTRACT**

In this paper, we constrain the properties of primordial binary populations in Galactic globular clusters. Using the MOCCA Monte Carlo code for cluster evolution, our simulations cover three decades in present-day total cluster mass. Our results are compared to the observations of Milone et al. (2012) using the photometric binary populations as proxies for the true underlying distributions, in order to test the hypothesis that the data are consistent with an universal initial binary fraction near unity and the binary orbital parameter distributions of Kroupa (1995). With the exception of a few possible outliers, we find that the data are to first-order consistent with the universality hypothesis. Specifically, the present-day binary fractions *inside* the half-mass radius can be reproduced assuming either high initial binary fractions near unity with a dominant soft binary component as in the Kroupa distribution combined with high initial densities ($10^4$-$10^6$ $M_\odot$ $pc^{-3}$), or low initial binary fractions ($\sim$ 5-10%) with a dominant hard binary component combined with moderate initial densities near their present-day values ($10^2$-$10^3$ $M_\odot$ $pc^{-3}$). This apparent degeneracy can potentially be broken using the binary fractions outside the half-mass radius - *only high initial binary fractions with a significant soft component combined with high initial densities can contribute to reproducing the observed anti-correlation between the binary fractions outside the half-mass radius and the total cluster mass.* We further illustrate using the simulated present-day binary orbital parameter distributions and the technique first introduced in Leigh et al. (2012) that the relative fractions of hard and soft binaries can be used to further constrain both the initial cluster density and the initial mass-density relation. Our results favour an initial mass-density relation of the form $r_h \propto M_{clus}^{\alpha}$ with $\alpha < 1/3$, corresponding to an initial correlation between cluster mass and density.

**Key words:** binaries: general – stars: kinematics and dynamics – globular clusters: general – stars: formation – methods: numerical.

## 1 INTRODUCTION

The origin of globular clusters (GCs) remains an open question. The initial conditions present during and after the gas-embedded phase are poorly constrained. For instance, were GCs formed during the monolithic collapse of a single massive giant molecular cloud, or are they the merged remnants of many lower mass sub-clumps and/or filamentary structures? Recent evidence suggests that globular clusters underwent prolonged star formation early on in their lifetimes (see Gratton, Carretta & Bragaglia (2012) for a recent review). That is, gas could have been present in significant quantities for the first $\sim 10^8$ years, albeit perhaps

⋆ E-mail: nleigh@ualberta.ca (NL); mig@camk.edu.pl (MG); mmarks@astro.uni-bonn.de (MM); webbjj@mcmaster.ca (JW); ahypki@camk.edu.pl (AH); heinke@ualberta.ca (CH); pavel@astro.uni-bonn.de (PK); asills@mcmaster.ca (AS)

© 2011 RAS

intermittently (Conroy & Spergel 2011; Conroy 2012). This evidence comes in the form of multiple stellar populations identified in the colour-magnitude diagram (e.g. Piotto et al. 2007), as well as curious abundance anomalies that cannot be explained by a single burst of star formation (e.g. Osborn 1971; Gratton et al. 2001). On the other hand, a prolonged gas-embedded phase seems to conflict with the recent findings of Bastian & Strader (2014), who report a lack of gas and dust in young massive clusters in the LMC and SMC, thought to be (possible) analogs of primordial Galactic GCs. In general, the presence of multiple populations in Galactic GCs is indicative of a complex formation history. For example, massive clusters could re-accrete gas after an initial burst of star formation, allowing for a new generation of stars to form (Pflamm-Altenburg & Kroupa 2007), or they might capture stars from the field in significant numbers if they are still forming in their natal molecular cloud (Pflamm-Altenburg & Kroupa 2009; Fellhauer, Kroupa & Evans 2006).

In Paper I of this series (Leigh et al. 2013a), we constrained the origin of the observed dependences of the present-day mass function (MF) slope and concentration parameter on the total cluster mass. By focusing on the role of dynamics in modifying these parameters over $\sim 12$ Gyr of evolution, we showed that the present-day global stellar MF variations are consistent with an universal initial MF modified by two-body relaxation and Galactic tides, but some initial correlation between the concentration parameter and the total cluster mass is needed to reproduce the present-day observed relations (a similar result was shown by Marks & Kroupa (2010) to explain the present-day relation between total cluster mass and concentration, but invoking primordial gas expulsion). We further showed that the present-day distributions of core binary fractions can be reproduced from an universal initial binary fraction of 10%, assuming an orbital period distribution that is flat in the logarithm of the semi-major axis combined with an appropriate choice of the initial cluster mass-radius relation. Importantly, however, this did not preclude other combinations of the initial binary fraction and orbital parameter distributions (i.e. the semi-major axis, mass ratio and eccentricity distributions).

Among the many uncertainties pertaining to the origins of GCs are the properties of their primordial binary populations. Much more is known about the *present-day* binaries in these clusters, identified as photometric binaries above the main-sequence in the colour-magnitude diagram (e.g. Milone et al. 2012), or at higher energies as exotic objects like low-mass x-ray binaries (LMXBs) (e.g. Hut, Murphy & Verbunt 1991), millisecond pulsars (MSPs) (e.g. Verbunt, Lewin & van Paradijs 1989) and cataclysmic variables (CVs) (e.g. Pooley & Hut 2006; Cohn et al. 2010). Blue straggler (BS) formation as well is thought to involve binary stars, whether it be due to mass-transfer within a binary, collisions during encounters involving binaries or even some triple-based mechanism (e.g. Leigh & Sills 2011; Geller et al. 2013) such as Kozai-induced mergers (e.g. Perets & Fabrycky 2009; Naoz & Fabrycky 2014). Despite the importance of these populations for understanding a number of astrophysical processes, little is known about their progenitor populations and the conditions from which they evolved.

The principal physical mechanisms driving the time evolution of the binary orbital parameter distributions in dense star clusters are two-body relaxation and direct encounters involving binaries.[1] Two-body relaxation drives mass segregation in clusters, causing binaries to drift in toward the cluster centre. This is due to the larger masses of binaries relative to single stars. That is, the tendency for clusters to evolve toward, on average, a state of energy equipartition (or, more accurately, energy equilibrium, although technically this idealized state is never fully reached in real clusters) results in a reduction in the speeds of the more massive binaries. Thus, two-body relaxation causes the inward radial migration of binaries in clusters, with the most massive binaries having the shortest mass segregation timescales (Vishniac 1978). Hence, this process does not directly impact the (global) binary orbital parameter distributions. Indirectly, however, mass segregation delivers binaries to the central cluster regions where the density is highest, and encounters typically occur on shorter timescales.[2] Binary encounters have a more direct effect on the binary orbital parameter distributions via exchanges, ionizations, hardening, softening, etc. (e.g. Marks & Kroupa 2012; Marks et al. 2014). For example, exchanges involve an interloping single star (or binary) that undergoes a resonant gravitational interaction with the components of a binary and, in the end, can cause one of the original binary members to be ejected (Hills 1975; Sigurdsson & Phinney 1993). To summarize, mass segregation delivers binaries to the core, where they are dynamically processed due to binary encounters (ignoring the possible binary burning phase in the evolution of young and dense clusters when binaries are destroyed on a crossing time (Marks, Kroupa & Oh 2011)).

The time evolution of the binary semi-major axis distribution in dense clusters can be reasonably well summarized using one simple rule, called the Hills-Heggie Law (Hills 1975; Heggie 1975). This relies on the concept of a "hard-soft" boundary, or the semi-major axis $a_{\rm HS}$ for which the binary orbital energy is equal to the average single star kinetic energy. That is:

$$a_{\rm HS} = \frac{G\bar{m}}{\sigma^2}, \tag{1}$$

where $\bar{m}$ is the average single star mass and $\sigma$ is the root-mean-square (rms) velocity. Here, an average binary is defined such that both components have masses equal to the average single star mass, and $\sigma$ is calculated using Equation 4-80b of Binney & Tremaine (1987) (hence it corresponds to the rms velocity at the half-light radius). Binaries with (absolute) orbital energies greater than that corresponding to the hard-soft boundary are called "hard", and typically experience a reduction in their semi-major axes upon undergoing encounters with single stars. "Soft" binaries, on the other hand, have orbital energies less than the average single star kinetic energy, and become even softer post-encounter as their semi-major axes typically increase. The softest binaries are easily ionized during encounters with single stars.

[1] We note that in the binary-burning phase of initially binary-dominated clusters, the initial crossing time is of crucial importance.

[2] Mass segregation can also cause the average object mass in the core to increase, which can in turn affect the hard-soft boundary.

Thus, the net effect of binary encounters is that hard binaries become harder, and soft binaries become softer.[3] This is the Hills-Heggie Law.

Recently, Milone et al. (2012) performed a photometric study of the main-sequence binary populations in a sample of 59 GCs. The authors confirmed a previously reported (Sollima et al. 2007) anti-correlation between the binary fraction and the total cluster mass. Sollima (2008) previously showed that this trend can arise naturally assuming an universal initial binary fraction. In this scenario, the anti-correlation appears due to the disruption of soft binaries in the cluster core, combined with the evaporation of single stars from the cluster outskirts (e.g. Duchêne, Bouvier & Simon 1999; Fregeau, Ivanova & Rasio 2009; Parker et al. 2009). The efficiency of the former process should increase with increasing cluster mass and density (Marks, Kroupa & Oh 2011), whereas the efficiency of the latter process is driven by two-body relaxation and should increase with decreasing cluster mass and density (i.e. $t_{rel} \propto M^{0.5} r_h^{1.5}$). This contributes to high binary fractions in low-mass cluster cores, and low binary fractions in high-mass cores.

Even more recently, Geller et al. (2013) showed using $N$-body simulations that the radial dependence of the binary frequency is quite sensitive to the dynamical age of a cluster. Dynamics initially destroys soft binaries in the core, giving rise to a binary frequency that rises toward the cluster outskirts. After approximately one half-mass relaxation time in clusters with an initial mass $10^4$-$10^5$ $M_\odot$, a bimodal radial binary frequency develops since binaries just outside the core have now drifted in due to mass segregation. The minimum in binary frequency extends radially outward as time goes on, finally giving way to a binary fraction that decreases with increasing clustercentric distance all the way to the tidal radius after $\sim 4-6$ (initial) half-mass relaxation times. Such a minimum in the binary fraction is clearly visible in NGC 5272 (M3), with a 6 Gyr half-mass relaxation time, around the half-mass radius (Milone et al. 2012). The (incomplete) data of the comparable cluster NGC 5024 is suggestive of a similar minimum, and a binary fraction minimum at 1-2 half-mass radii is visible in the clusters NGC 6584 and 6934, which have relaxation times of 1 Gyr. An analogous bimodality has been observed in BS populations, and it is likely that mass segregation is again responsible for this (possibly transient; Hypki, A., 2014, PhD thesis) feature (Ferraro et al. 2012).

In this paper, the second of the series, we delve further into the issue of the initial binary properties in globular clusters. In particular, we explore whether or not the observed present-day distribution of Galactic GC binary fractions can be reproduced assuming an universal initial binary fraction of 95% combined with the binary orbital parameter distributions taken from Kroupa (1995a) (i.e. with a significant fraction of soft binaries), which are deduced from present-day star-forming regions in the Milky Way disk and its field population. We also explore different initial mass-density relations, but all of these correspond to relatively high initial densities ($\sim 10^4$-$10^6$ $M_\odot$ pc$^{-3}$). To do this, we generate a series of simulations for GC evolution performed using the MOCCA code (Giersz et al. 2013), and compare the results to the presently observed binary fractions of Milone et al. (2012).

Importantly, there may never be an instant in time when the initial binary distribution functions are fully established. In a dense star-forming environment, binaries form but can be dissociated into individual stars before other binaries form. The binary population is constantly changing due to break-ups and mergers. However, mathematically convenient initial binary distribution functions can be deduced from young stellar populations. Crucially, the prior dynamical processing of the normalizing population must be properly accounted for. This was first done by Kroupa (1995a) using constraints given by old populations. The resulting mathematical formalism can be viewed as that which an ideal population would populate if it could. For example, in an extreme star-burst that forms a very dense massive cluster, wide binaries cannot really form. In this case, a binary fraction of 100% seems unphysical. But, we can model this using our derived mathematical description of primordial binary populations, since they become naturally truncated by the dynamical configuration of the cluster. Thus, the same initial binary distribution functions can be adopted, subject to the local cluster conditions. These are taken care of naturally in any $N$-body or Monte Carlo model for GC evolution, leading to some slight cooling of the initial cluster configuration due to the disruption of wide binaries, although this typically represents at most a small fraction of the total energy budget of the cluster (Leigh et al. 2013a).

In Section 2, we present our Monte Carlo models for GC evolution performed using MOCCA, along with our chosen initial conditions. In Section 3, we present our results and compare them to the observations. We further describe our method, adapted from Leigh et al. (2012), for extrapolating from only a handful of models convenient equations for the predicted present-day distributions of orbital energies for a range of present-day total cluster masses (spanning three orders of magnitude). This allows us to efficiently study and compare the evolution of our model binary populations in energy-space, as a function of different initial cluster densities. Finally, in Section 4, we discuss the implications of our results for primordial binaries in Milky Way GCs.

## 2 MODELS

In this section, we describe the Monte Carlo code called MOCCA used to simulate the cluster evolution, and describe our choice of initial conditions. MOCCA is ideal for studies of globular cluster evolution spanning a range of initial conditions, given its fast and robust coverage of the relevant parameter space (e.g. Giersz et al. 2013).

### 2.1 Monte Carlo models: MOCCA

We use the MOCCA code to produce all of our simulated clusters. It combines the Monte Carlo technique for cluster evolution (Henon 1971) with the FEWBODY code

[3] This statement relies on averages. In reality, a binary that would be classified as hard according to Equation 1 can actually be soft during a particularly energetic encounter. Or, binaries classified as soft by Equation 1 can be hard if the component masses are larger than the average stellar mass.

(Fregeau et al. 2004) to perform numerical scattering experiments of small-number gravitational interactions. The code relies on analytic formulae for stellar evolution taken from Hurley, Pols & Tout (2000), and performs binary evolution calculations using the BSE code (Hurley, Pols & Tout 2002). The MOCCA simulations are performed on a PSK2 cluster at the Nicolaus Copernicus Astronomical Centre in Poland. Each simulation is run on one CPU, and the cluster is based on AMD Opteron processors with 64-bit architecture (2-2.4 GHz). For further information about the MOCCA code, see Hypki & Giersz (2013), Giersz et al. (2013) and Leigh et al. (2013a).

### 2.2 Initial conditions

For every choice of Galactocentric radius and initial cluster structure, we run models having a total cluster mass of $10^4$, $5 \times 10^4$, $10^5$, $5 \times 10^5$ and $8 \times 10^5$ $M_\odot$ initially. All models begin with a global initial binary fraction $f_b = 95\%$,[4] and we do not assume any primordial binary (or stellar) mass segregation in our models. The initial binary orbital parameter distributions are taken from Equation 46 of Kroupa et al. (2013). Therefore, initial eccentricities follow a thermal distribution $f_e(e) = 2e$. The initial binary mass function is derived from random pairing in the mass range 0.08 to 5 $M_\odot$, and favouring mass ratios near unity above 5 $M_\odot$. The initial period distribution function is:

$$f_P = \eta \frac{\log_{10} P - \log_{10} P_{min}}{\delta + (\log_{10} P - \log_{10} P_{min})^2}, \quad (2)$$

where $\eta = 2.5$, $\delta = 45$ and $\log_{10}P_{min} = 1$. The normalization $\int f_P d(\log_{10}P) = 1$ (where the lower and upper limits of integration are, respectively, $\log_{10}P_{min}$ and $\log_{10}P_{max}$, with $\log_{10}P_{max} = 8.43$ and P is in days) is imposed for a binary fraction of unity.[5] The assumption of high binary fractions near unity maximizes the statistical significance of our analysis of the evolution of the binary populations in energy-space. Additionally, previous work (Marks & Kroupa 2012; Marks et al. 2014) showed that such a high binary fraction is needed to obtain the required agreement with the observed binary fractions in young Galactic open clusters, when combined with our choice of orbital parameter distributions (Kroupa 1995a,b; Kroupa et al. 2013) and high initial densities (see below).

We run models at Galactocentric radii $R_{GC}$ of 4 kpc, 8 kpc and 10 kpc, all with circular orbits in the Galactic potential. To model the Galactic potential, MOCCA assumes a point-mass with total mass equal to the enclosed Galaxy mass at $R_{GC}$. As described in (Giersz et al. 2013), the criterion used to define the escape rate of stars and binaries from the cluster is taken from Fukushige & Heggie (2000), and accounts for the possibility that objects with energies greater than the local escape energy can be scattered back into the cluster to become re-bound (Baumgardt 2001). All models are evolved for 12 Gyr.[6]

We adopt an initial mass function (IMF) taken from Kroupa, Tout & Gilmore (1993) in the mass range 0.08 - 100 $M_\odot$. That is, we assume a mass function of the form $\xi(m) \propto m^{-\alpha}$, with $\alpha = 2.7$ for stars with masses $m \geqslant 1$ $M_\odot$, $\alpha = 2.2$ for stars with masses in the range $0.5 \leqslant m/M_\odot < 1$, and $\alpha = 1.3$ for stars with masses in the range $0.08 \leqslant m/M_\odot < 0.5$. We also check that our results are roughly[7] insensitive to our choice of IMF by re-running all models with a two-segmented Kroupa IMF taken from Kroupa (2008). We assume a metallicity of $Z = 0.001$ for all models. Initial conditions for all models are summarized in Table 1.

For all models, we adopt a King density profile with initial concentration $W_0 = 6$. All models are either initially tidally filling or under-filling. The degree of under-filling is set by the parameter $f_{und} = r_t/r_h$, where $r_t$ and $r_h$ are the tidal and half-mass radii, respectively. For tidally-filling models, the parameter $f_{und}$ is defined by the initial concentration $W_0$. We consider mass-radius relations of the form $r_h = \beta M_{clus}^{\alpha}$ for some constants $\beta$ and $\alpha$. For the initially tidally-filling models, we adopt $\alpha = 1/3$, corresponding to a constant initial density for every set of models with the same initial conditions (but different initial total cluster masses).[8] For the initially tidally-underfilling models, we adopt a slightly smaller value $\alpha \lesssim 1/3$, corresponding to initial densities that increase slightly (i.e. less than a factor of two) with increasing initial cluster mass. For the tidally-filling and tidally-underfilling models, the corresponding initial densities range from $\sim 10-100$ $M_\odot$ $pc^{-3}$ and $\sim 10^4$-$10^6$ $M_\odot$ $pc^{-3}$, respectively, inside the half-mass radius.

### 2.3 "Observing" the models

In order for comparisons to the observed data to be meaningful, the simulated cluster properties must be calculated analogously to the observed values from Milone et al. (2012). That is, we must "observe" the simulated clusters in the same way as was done for the observations. To this end, both the core and half-light radii are calculated from the 2-D surface brightness profiles of the models. The core radius is defined as the distance from the cluster centre at which the surface brightness falls to half its central value, and the half-light radius is defined as the distance from the cluster centre containing half the total cluster luminosity.[9] We further ensure that the binary fractions are consistently calculated over the range of binary mass ratios ($q > 0.5$) and MS stellar masses (0.47 - 0.76 $M_\odot$) used to derive the observed values.

[4] We restrict ourselves to a binary fraction slightly less than unity to avoid computational problems that arise in MOCCA if the number of single stars is initially zero.

[5] Note that all logarithms in this paper are to the base 10.

[6] Models with an initial mass $10^4$ $M_\odot$ do not survive the full 12 Gyr, dissolving after $\sim 10-11$ Gyr of cluster evolution.

[7] Our results do slightly change assuming a two-segmented Kroupa IMF relative to the three-segmented case, since the former models undergo more stellar evolution-induced mass loss early on due to having a larger fraction of high-mass stars. This enhanced mass loss can result in a slightly accelerated cluster evolution, yielding final binary fractions at 12 Gyr that are slightly lower (by $\sim 1\%$) than we find adopting a three-segmented IMF.

[8] Note that $\beta \propto f_{und}^{-3} R_{GC}^3$ if $\alpha = 1/3$, where $R_{GC}$ is the Galactocentric distance.

[9] We have checked that our results hold qualitatively using instead the 3-D (i.e. deprojected) radii and number counts.

| Total Cluster Mass (in $M_\odot$) | Time (in Gyr) | $R_{GC}$ (in kpc) | $f_{und}$ | Binary Fraction | Symbol |
|---|---|---|---|---|---|
| 10000 | 10-11 | 10 | 6.8 | 95 | Open circle |
| | | | 50.0 | | Filled circle |
| | | 8 | 6.8 | | Open square |
| | | | 50.0 | | Filled square |
| 50000 | 12 | 10 | 6.8 | 95 | Open circle |
| | | | 50.0 | | Filled circle |
| | | 8 | 6.8 | | Open square |
| | | | 50.0 | | Filled square |
| 100000 | 12 | 10 | 6.8 | 95 | Open circle |
| | | | 50.0 | | Filled circle |
| | | 8 | 6.8 | | Open square |
| | | | 50.0 | | Filled square |
| 500000 | 12 | 10 | 6.8 | 95 | Open circle |
| | | | 50.0 | | Filled circle |
| | | 8 | 6.8 | | Open square |
| | | | 50.0 | | Filled square |
| | | | 100.0 | | Open pentagon |
| | | 4 | 6.8 | | Open triangle |
| | | | 50.0 | | Filled triangle |
| | | | 100.0 | | Filled pentagon |
| 800000 | 12 | 10 | 6.8 | 95 | Open circle |
| | | | 50.0 | | Filled circle |
| | | 8 | 6.8 | | Open square |
| | | | 50.0 | | Filled square |
| | | | 100.0 | | Open pentagon |
| | | 4 | 6.8 | | Open triangle |
| | | | 50.0 | | Filled triangle |
| | | | 100.0 | | Filled pentagon |

**Table 1.** Initial conditions for all Monte Carlo (MOCCA) models.

## 3 RESULTS

In this section, we present the results of our MOCCA simulations for globular cluster evolution. We begin by comparing the simulated binary fractions for *all* models to the observed binary fractions taken from Milone et al. (2012), both inside and outside the half-mass radius. We then apply our extrapolation technique from Leigh et al. (2012) to two sets of models, each with a different initial mass-radius relation (and hence different initial density) which we refer to as the tidally-filling and tidally-underfilling cases. *Note that we refer to each group of models with the same initial binary fraction, orbital parameter distributions and mass-radius relation (defined either by whether or not the clusters are initially tidally-filling or tidally-underfilling, and the Galactocentric distance), but different initial total cluster masses, as a "set".*

### 3.1 Comparisons to the observed binary fractions

Figure 1 compares the simulated and observed present-day binary fractions, both inside (blue points) and outside (red points) the half-mass radius (see the figure caption for an explanation of which symbols correspond to which models). To calculate the observed binary fractions inside $r_h$ from the data provided in Milone et al. (2012), we use the relation:

$$f_{b,h} = \frac{f_{b,c} M_c + f_{b,ch}(M_h - M_c)}{M_h}, \qquad (3)$$

where $f_{b,c}$ is the core binary fraction, $f_{b,ch}$ is the binary fraction in the annulus between the core and half-mass radii, $M_c = 4\pi r_c^3 \rho_c/3$ is the mass within the core (assuming a mass-to-light ratio of 2 for all GCs to convert the central luminosity densities given in Harris (1996, 2010 update) to central mass densities) and $M_h = M_{clus}/2$ is the total mass inside the half-mass radius (and we have assumed that the average single star mass $\bar{m}$ is the same everywhere within $r_h$, and the average binary mass is $2\bar{m}$). Importantly, we performed the subsequent analysis using all available binary fractions ($f_{b,c}$, $f_{b,ch}$ and $f_{b,t}$), instead of just the binary fractions inside and outside $r_h$, to verify that our key conclusions remain unchanged.

As is clear from Figure 1, the initially tidally-filling models yield binary fractions at 12 Gyr that are larger than the observed binary fractions by a factor of a few (i.e. $\sim$ 2-4) for our choice of initial binary fraction (i.e. 95%). This is no surprise, because binary disruption is too inefficient in such initially extended clusters with such high binary fractions, even with a significant soft binary component. The initially tidally-underfilling models, however, yield present-day binary fractions that agree quite well with the observed range, both inside and outside the half-mass radius. This illustrates that a high initial cluster density ($\sim 10^4$-$10^6$ $M_\odot$ pc$^{-3}$ at the half-mass radius, relative to $\sim 10-100$ $M_\odot$ pc$^{-3}$ for the tidally-filling models) is needed to reproduce the observed present-day binary fractions for our choice of orbital parameter distributions *if* the initial binary fraction was near unity. This is similar to the results found in Marks, Kroupa & Oh

(2011), however the initial densities required by our models are lower than those in Marks, Kroupa & Oh (2011) by at least two orders of magnitude (i.e. initial densities on the order of $\sim 10^8$ $M_\odot$ $pc^{-3}$). This discrepancy can be accounted for by the inclusion of the two-body relaxation phase of cluster evolution in MOCCA, not accounted for by Marks, Kroupa & Oh (2011).

Importantly, this proves neither that the initial density was indeed high, nor that the initial binary fractions were close to unity. For example, in Leigh et al. (2013a), we showed that the present-day central binary fractions can be reproduced assuming an universal initial binary fraction of 10% and a period distribution flat in the logarithm of the binary semi-major axis, as suggested by Sollima (2008). Thus, our results *for the binary fractions inside* $r_h$ demonstrate only that the presently available data for Milky Way GC binary fractions are roughly consistent with an initial binary fraction near unity, in addition to an universal set of initial binary orbital parameter distributions resembling that of Kroupa (1995b) (and in Kroupa et al. 2013), provided the initial mass-radius relation is chosen to ensure a sufficiently high initial cluster density. Our results for the binary fractions *outside* $r_h$ tell a different story, however. The key feature in Figure 1 we wish to draw the reader's attention to is that the *high initial densities adopted in the tidally-underfilling models are needed to reproduce the anti-correlation between* $f_{b,t}$ *and the total cluster mass seen in the observed data*, at least for our choice of initial conditions.[10] Indeed, for the tidally-filling models, a *correlation* is obtained between $f_{b,t}$ and $M_{clus}$ at 12 Gyr. Thus, even if we were to lower the initial binary fractions in the tidally-filling models to ensure better agreement between the simulated binary fractions inside $r_h$ and the observations, we would still fail to reproduce the observed dependence of $f_{b,t}$ on $M_{clus}$ (i.e. outside the half-mass radius). We will return to this important point in Section 4.

More quantitatively, we obtain lines of best-fit for the observed and simulated relations. To do this, we first convert the observed and simulated binary fractions to number counts, both inside and outside the half-mass radius, and then perform least-squares fits to the data. The conversion to number counts introduces some additional uncertainty in the comparison between the models and observations that we are not able to accurately quantify. Consequently, we limit ourselves to a qualitative discussion of the uncertainties for the fit parameters. The lines of best-fit are shown in Figure 2 for the observations, for which we obtain a sub-linear slope of 0.58 both inside and outside the half-mass radius (and y-intercepts of 0.92 and 0.79, respectively). The slopes we find for the models tend to be much higher, except for the densest models at 4 kpc (see the filled pentagons in Figure 2). This is further evidence that *high initial densities are needed to reproduce the observations for our choice of initial conditions.* Importantly, we note that the correlations are stronger for the models than for the observed data, with significant scatter about the lines of best-fit. This is to be expected since, for example, we adopt the same Galactocentric distance for every set of models (i.e. with the same initial conditions but different initial cluster masses), and circular orbits. Real Galactic GCs, however, show a range of Galactocentric distances, and often deviate significantly from circular orbits (e.g. Webb et al. 2013, 2014). Some of the scatter is also stemming from the fact that the dynamical (and absolute) ages of Galactic GCs do not scale completely smoothly with total cluster mass (even assuming an universal initial mass-density relation) due to, for example, a variable tidal field (Webb et al. 2014).

At 12 Gyr, the half-mass radii are roughly the same as their initial values for the tidally-filling models, whereas they have increased by a factor of $\sim$ 3-7 in the tidally-underfilling models. Simultaneously, the total cluster masses have dropped by a factor of a few in both cases, albeit slightly more so for the tidally-filling models (by a factor of about two). It follows that, by 12 Gyr, the mean densities inside $r_h$ have dropped by a factor of $\sim$ a few and a couple orders of magnitude, respectively, for the tidally-filling and tidally-underfilling models. Thus, at 12 Gyr, it is the initially tidally-underfilling models that best reproduce the observed densities of Galactic GCs. For example, for our models at 10 kpc, the mean densities inside $r_h$ are an order of magnitude higher in the tidally-filling models (i.e. $\sim$ 100 $M_\odot$ $pc^{-3}$) than in the tidally-underfilling models (i.e. $\sim$ 10 $M_\odot$ $pc^{-3}$). At 4 kpc, these densities are about an order of magnitude higher at 12 Gyr, however the difference between the tidally-filling and tidally-underfilling models remains about the same (i.e. an order of magnitude). Thus, the present-day mean density inside the half-mass radius offers another means of constraining the initial cluster density. Indeed, the observed present-day mean densities inside $r_h$ are typically in the range $\sim 10^2$-$10^3$ $M_\odot$ $pc^{-3}$, which seem to agree better with our initially tidally-underfilling models.

But can we simultaneously reproduce the correct binary fractions both inside and outside the half-mass radius in all clusters? To address this question, Figure 3 compares the ratio of the simulated and observed binary fractions inside and outside the half-mass radius, or $f_{b,h}/f_{b,t}$. The symbols are the same as in Figure 1, and we include a (dotted) line to highlight a ratio of unity. Figure 3 illustrates that our models (both the tidally-filling and tidally-underfilling models) do indeed roughly reproduce the range of ratios $f_{b,h}/f_{b,t}$ observed in *most* Galactic GCs, with the exception of a few outliers. We note a shallow but clear anti-correlation between the total (present-day) cluster mass and the ratio $f_{b,h}/f_{b,t}$ in the simulations, which is much weaker (but arguably still present) in the observations (ignoring the outliers). This is in rough agreement with the results of Fregeau, Ivanova & Rasio (2009), namely that the binary fraction at the half-mass radius remains about constant as clusters evolve, while the binary fractions inside and outside the half-mass radius slowly increase and decrease, respectively. Thus, the ratio $f_{b,h}/f_{b,t}$ should increase with increasing dynamical age.

Some of the more massive Galactic GCs in our sample have $f_{b,h}/f_{b,t} < 1$, while also being slightly lower than we are able to reproduce in any of our models. For example, NGC 6205 and NGC 5272 have the lowest values of the ratio $f_{b,h}/f_{b,t}$, with values of 0.48 and 0.68, respectively. With the exception of NGC 6205, all of these clusters have binary fractions inside the core that exceed their binary fractions in

[10] Our results do not necessarily exclude all other combinations of initial conditions, only that these initial conditions are able to match the observations at 12 Gyr.

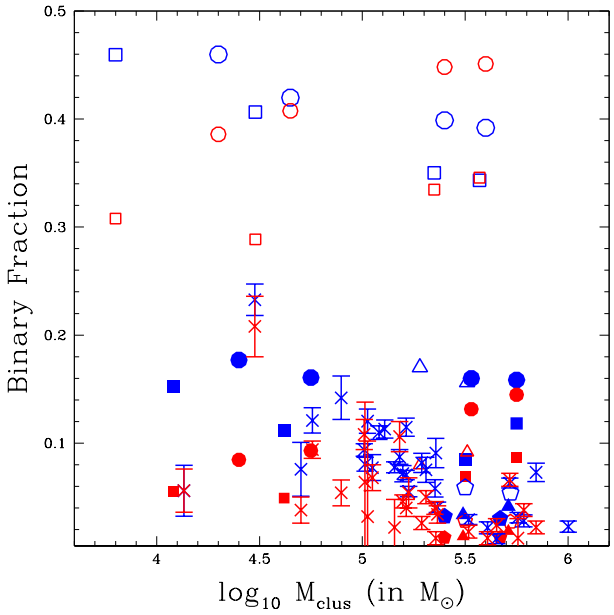


**Figure 1.** The simulated binary fractions are shown for all models at 12 Gyr as a function of the total cluster mass (in $M_\odot$) at 12 Gyr, both inside (blue points) and outside (red points) the cluster half-mass radius. Initially tidally-filling and tidally-underfilling models are indicated by the open and filled symbols, respectively. Models at 10 kpc, 8 kpc and 4 kpc are shown by the circles, squares and triangles, respectively. Models with $f_{und} = r_t/r_h = 100$ initially (i.e. even more tidally-underfilling than our standard tidally-underfilling models) are shown by the pentagons for models evolved both at 8 kpc (open symbols) and 4 kpc (filled symbols). The observed binary fractions taken from Milone et al. (2012) and/or calculated in Leigh et al. (2013b) are indicated by the crosses, and error bars show the corresponding uncertainties where available.

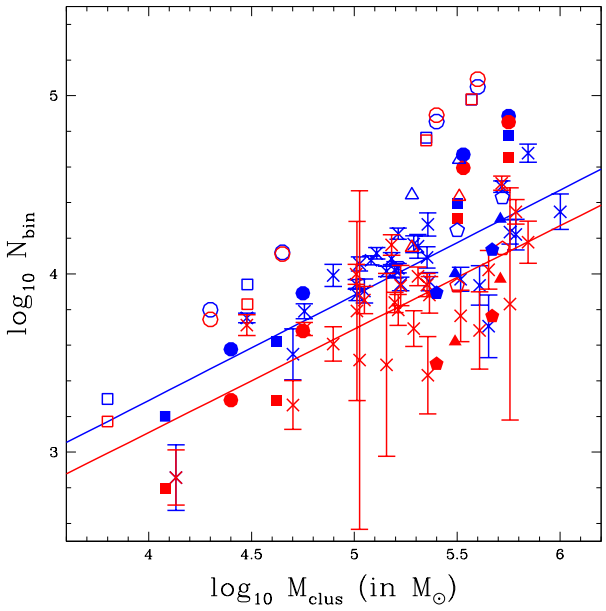


**Figure 2.** The (logarithm of) the number of binaries are shown for all models as a function of the total cluster mass at 12 Gyr. The symbols used to represent each model are the same as in Figure 1, and the observed numbers are again indicated by the crosses. Lines of best-fit are shown by the solid lines for the observations only, both inside (blue) and outside (red) the half-light radius. Error bars are calculated using the binary fraction uncertainties from Milone et al. (2012).

the annulus separating the core and half-mass radii (which typically a few parsecs thick and constitutes $\sim 40\%$ of the total cluster mass). Hence, the ratio $f_{b,h}/f_{b,t}$ is artificially decreased in these clusters due to our calculation of $f_{b,h}$ in Equation 3 combined with the fact that the volume of the core is much smaller than that of the annulus separating the core and half-mass radii. In all but two of these clusters, the binary fraction in the core is greater than that outside the half-mass radius. The exceptions to this are NGC 6101 and NGC 6205. These clusters have half-mass relaxation times of a few Gyr (Harris 1996, 2010 update), which could contribute to low dynamical ages for these clusters and hence high binary fractions outside $r_h$ at 12 Gyr. At the same time, these clusters could host a large proportion of soft binaries that are easily disrupted in the higher density central cluster regions, which would contribute to low binary fractions inside $r_h$ (Geller et al. 2013). [11] Given that in these two clusters the ratio $f_{b,h}/f_{b,t}$ is only slightly smaller than seen in our models with the highest initial densities, this discrepancy can partially be corrected by adopting slightly higher initial concentrations (e.g. Leigh et al. 2013a), or if these clusters recently underwent a phase of core-collapse (although their present-day concentrations do not seem to suggest this). Having said that, in our models, the exact cluster age at which core-collapse first occurs is sensitive to the initial random seed, and core-collapse does not occur in any of our simulated clusters. Therefore, given that the discrepancy is small, our simulations could possibly reproduce the observed ratio $f_{b,h}/f_{b,t}$ in either NGC 6101 or NGC 6205 with the right random seed. This requires verification in future work.

Interestingly, $\sim 4$ Galactic GCs in our sample show $f_{b,h}/f_{b,t}$ values that are higher than any reproduced by our models. Basic theory cannot explain this discrepancy since extrapolating the results of our models to higher initial concentrations should yield lower values for the ratio $f_{b,h}/f_{b,t}$. We will return to this curious result in Section 4. For now, we note that, when the observational error bars are considered, only one of these 4 clusters is discrepant with our models, namely NGC 5927.

### 3.2 Quantifying the degree of dynamical processing in energy-space

In this section, we consider how the underlying binary orbital parameter distributions are affected by dynamical processing. In this regard, what we are able to learn from the binary fractions alone is limited. Specifically, binary fractions can only tell us about the degree of dynamical processing if we know a priori what were the initial binary fractions and cluster conditions. The evolved distributions of binary orbital parameters (if available), on the other hand, tell a more detailed story.

In the subsequent sections, we describe our technique for extrapolating the binary orbital parameter distributions obtained at 12 Gyr to any cluster mass using only a handful of models. The method is adapted from Leigh et al. (2012), and is meant to facilitate more efficient coverage of the relevant parameter space, and ultimately simulate a larger range of initial conditions for comparison to the observed data while minimizing the total computational expense. We apply this technique to the results of our models in order to better study *which* binaries are most affected by dynamical processing, for our choice of initial binary orbital parameter distributions.

#### *3.2.1 Description of the extrapolation technique*

First, both the rates of two-body relaxation and binary encounters depend on the total cluster mass and density. Specifically, the rate of two-body relaxation increases with decreasing cluster mass and increasing density, whereas the rate of binary encounters increases with increasing cluster mass and increasing density (ignoring the dependence on the present-day binary fraction, which also scales with the cluster mass as, for example, $f_{b,core} \propto M_{core}^{-0.4}$) (e.g. Sollima 2008; Milone et al. 2012; Leigh et al. 2013b). Moreover, the hard-soft boundary is primarily determined by the cluster velocity dispersion, which in turn is determined by the total cluster mass via the virial theorem (if the cluster is in virial equilibrium, i.e. sometime after the gas-embedded phase). In fact, the rates of two-body relaxation and binary encounters should depend *solely* on the total cluster mass *if some initial mass-radius and mass-concentration relations are clearly defined* (assuming as well that the initial mass function and binary properties are either universal or depend directly on the total cluster mass). It follows from this key assumption that the time evolution of the binary orbital parameter distributions also depend directly on the total cluster mass. Thus, assuming universal initial distributions, the present-day binary orbital parameter distributions should vary *smoothly* with total cluster mass *for any set of coeval clusters*.

Next, we describe how we exploit this strong cluster mass-dependence through our extrapolation technique. This is feasible for Galactic globular clusters, since they all have roughly the same age (to within roughly a couple Gyr) (e.g. Salaris & Weiss 2002; De Angeli et al. 2005; Marin-Franch et al. 2009; Hansen et al. 2013), but not necessarily the same dynamical age. We emphasize that, for every set of models (i.e. with the same initial conditions but different total cluster masses), the initial values for all model parameters (e.g. the mass-density relation, the IMF, the Galactocentric distance, etc.) are chosen to ensure that the rates of two-body relaxation and binary encounters, and hence the present-day cluster-to-cluster differences in the binary orbital parameter distributions, depend solely on the total cluster mass. In other words, the dynamical ages for every set of models sharing the same initial conditions depend only on the total cluster mass.

We begin by converting the present-day binary orbital parameter distributions into orbital energy distributions. This is because, as described in Section 1, binary encounters most directly affect the binary orbital parameter distributions in energy space, whereas two-body relaxation does not care about the binary orbital parameters (only the total binary mass). Then, we bin the present-day orbital energy

[11] This is especially true if clusters are near a state of core-collapse (either just before, during and especially after), which can drastically increase the rate of binary disruption near the cluster centre. In fact, the number of primordial binaries can become very low, such that the number of newly formed binaries begins to outweigh it.

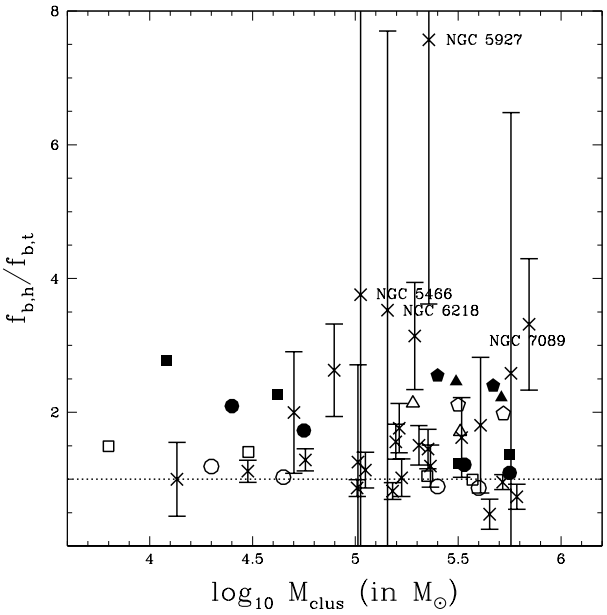


**Figure 3.** The ratio $f_{b,h}/f_{b,t}$ at 12 Gyr is shown for all models as a function of the total cluster mass, where $f_{b,h}$ and $f_{b,t}$ denote the binary fractions inside and outside the cluster half-mass radius, respectively. The symbols used to represent each model are the same as in Figure 1, and the observed ratios are again indicated by the crosses. Error bars are calculated using the observed binary fraction uncertainties provided in Milone et al. (2012). The dotted line indicates a ratio of unity between the inner and outer binary fractions.

distributions such that the bin sizes are equal in log-space, each spanning 1 dex. This is done for every model, and then models with the same initial conditions are grouped together. Hence, each group contains 5 models, each with a different initial total cluster mass but otherwise identical initial conditions.

Now, in order to quantify cluster-to-cluster differences in the present-day orbital energy distributions, we normalize the distributions by dividing each orbital energy by the average single star kinetic energy in the cluster at 12 Gyr, or $E_{avg} = 0.5 m \sigma^2$, where m is the average single star mass (taken to be 0.35 $M_\odot$ for all models, since the average mass is within the range 0.3 - 0.4 $M_\odot$ at 12 Gyr in all models) and $\sigma$ is the root-mean-square velocity (Binney & Tremaine 1987):

$$\sigma = \left(\frac{2GM}{5r_h}\right)^{1/2}, \quad (4)$$

where M is the total cluster mass and $r_h$ is the half-mass radius. Thus, in log-space, a *normalized* value for the orbital energy of 0 corresponds to the hard-soft boundary in each cluster. Next, we obtain for each group of models (with the same initial conditions but different initial total cluster masses) lines of best-fit for (the logarithm of) the number of binaries belonging to each orbital energy bin versus (the logarithm of) the total number of binaries spanning *all* energy bins, which corresponds to the total number of binaries in a given cluster.[12] This can be written:

$$\log_{10} N_{en,i} = \gamma_i \log_{10} N_{bin} + \delta_i, \quad (5)$$

where $N_{en,i}$ is the number of binaries belonging to orbital energy bin $i$, $N_{bin}$ is the total number of binaries in the cluster at 12 Gyr (i.e. spanning all orbital energy bins), and $\gamma_i$ and $\delta_i$ are both constants.

If the fraction of binaries belonging to each orbital energy bin, or $f_{en,i} = N_{en,i}/N_{bin}$, is constant for all cluster masses, then we would expect $N_{en,i}$ to scale linearly with $N_{bin}$. Or, equivalently, $\gamma_i \sim 1$ in Equation 5. However, if there is any systematic dependence of $f_{en,i}$ on the total cluster mass, then we should find that $N_{en,i}$ does *not* scale linearly with $N_{bin}$. In log-log space, the slope of the line of best-fit for orbital energy bin $i$ should be less than unity (i.e. $\gamma_i < 1$) if $f_{en,i}$ systematically decreases with increasing cluster mass. Conversely, we expect $\gamma_i > 1$ if $f_{en,i}$ systematically increases with increasing cluster mass. *Therefore, the exact values of $\gamma_i$ and $\delta_i$ are sensitive to the initial cluster conditions, in particular the initial binary orbital parameter distributions as well as the initial cluster density (i.e. the assumed mass-radius relation).*

Our motivation for adopting this technique is as follows. Equation 5 quantifies, for any cluster mass, the number of binaries belonging to each orbital energy bin as a function of the total number of binaries. The exact values of the parameters in Equation 5 are sensitive to the adopted initial binary orbital parameters and initial mass-density relation. Equation 5 can be converted into an equation that provides the

[12] We also repeat this procedure using only those binaries that satisfy the observational criteria of Milone et al. (2012), however our results are qualitatively the same.

number of binaries in each orbital energy bin as a function of the total number of *stars* using the total binary fraction, or $N_{bin} = f_b N$, where $f_b$ is the number of objects that are binaries and N is the total number of objects in the cluster (i.e. single stars and binaries). In turn, this can be converted into an expression that depends on the total cluster mass $M_{clus}$ using the simple relation $M_{clus} = mN$. Thus, Equation 5 effectively provides a means of quantifying cluster-to-cluster differences in the distribution of binary orbital energies as a function of the total (present-day) cluster mass. It follows from this that, within the universality hypothesis (i.e. adopting universal initial binary properties and an universal initial mass-density relation), knowing only the present-day observed total cluster mass and binary fraction, one can infer the underlying distributions of orbital energies for some assumed set of initial conditions. This is qualitatively similar to the technique presented in Marks, Kroupa & Oh (2011) for young star clusters at ages between 0-5 Myr. *Although we only apply the technique presented in this paper to two particular sets of initial conditions, in principle it can be done for any set of universal initial binary properties and mass-density relations.*

### *3.2.2 Application of the extrapolation technique*

In this section, we apply our extrapolation technique to two particular sets of models as a proof-of-concept, each with a different initial mass-density relation but otherwise identical initial conditions. The densest models are initially tidally-underfilling whereas the sparsest models are initially tidally-filling, and all models are evolved at a Galactocentric distance of 10 kpc. We remind the reader that we adopt an initial binary fraction of 95% for all models. This serves to maximize the final binary number counts at 12 Gyr. This is particularly important in those models with the highest initial densities (i.e. the tidally-underfilling models), since a significant number of soft binaries are disrupted very early on in the cluster lifetime (before the clusters have had enough time to expand to fill their tidal radii), causing the number of single stars to rapidly increase along with a corresponding decrease in the binary fraction. Additionally, we consider *all* binaries in this section, as opposed to just those binaries along the MS.

Figure 4 shows normalized histograms of the binary orbital energy distributions both initially (top panel) and at 12 Gyr, both for the tidally-filling (middle panel) and tidally-underfilling (bottom panel) models. As is clear from a comparison of the three panels in Figure 4, dynamical processing acts to reduce the number of soft binaries, increasing the fraction of hard binaries in the cluster. This effect is the most dramatic for the tidally-underfilling case, since the initial densities were the highest. Importantly, this result is roughly insensitive to the initial binary fraction due to our normalization technique (which removes the dependence on absolute numbers). Additionally, for every set of initial conditions, it is the most massive models that end up the most depleted of binaries, as expected.

Lines of best-fit are obtained using Equation 5 for each bin in orbital energy and provided in Table 2. These lines are shown in Figures 5 for the initial distributions (i.e. t = 0) as well as for both the tidally-filling and tidally-underfilling models at 12 Gyr.

One of the key features characteristic of Figures 4 and 5 is that *the fraction of hard binaries increases with decreasing total cluster mass,* and this effect becomes increasingly significant the more dynamical processing a binary population undergoes. This is illustrated in Figure 4 through our normalization method, since we see a clear trend for orbital energy bins with $\log_{10}(E_{orb}/E_{avg}) > 0$ (i.e. hard binaries) to become increasingly populated as more dynamical processing occurs. Similarly, a higher initial density results in a larger range of slopes and y-intercepts for our lines of best-fit over the six bins in orbital energy shown in Figure 5. This is evident from Table 2 upon comparing the range of slopes and y-intercepts for the tidally-filling (1.61 to 0.77 and -4.73 to -0.03 for the slopes and y-intercepts, respectively) and tidally-underfilling (2.39 to 0.19 and -9.20 to 2.67) models. This larger range of slopes and y-intercepts seen in initially denser clusters (i.e. the tidally-underfilling models) is due to a corresponding increase in the degree of dynamical processing, which in turn contributes to the fraction of hard binaries at 12 Gyr increasing more steeply with decreasing total cluster mass. This is the direct result of our assumed initial mass-density relation. Specifically, we assume a mass-density relation corresponding to a constant initial density for every set of models (i.e. with the same initial conditions). It follows from this that the encounter rate scales as $\Gamma \propto M_{clus}^{-1}$. Including the dependence of the encounter rate on the binary fraction only steepens the inverse mass-dependence further, since $\Gamma \propto f_b$ and the binary fraction is anti-correlated with the total cluster mass (Sollima 2008; Milone et al. 2012). Thus, the rate of dynamical processing is fastest in the least massive clusters for every set of models sharing the same initial conditions. Consequently, the rate of soft binary disruption is also the highest in the lowest mass clusters, causing the fraction of hard binaries to increase with decreasing cluster mass. Said another way, for a given orbital energy bin, the mean separation is larger in less massive clusters, which contributes to a shorter binary encounter time. This is because our normalization relies on dividing by the orbital energy corresponding to the hard-soft boundary, which is at larger orbital energies (i.e. less negative) in less massive clusters. This effect is the most significant in the initially tidally-underfilling models, since they have the highest initial densities and hence the highest encounter rates.

To summarize, without the need to do additional simulations to increase our range of simulated cluster masses, we now know the number of binaries in each orbital energy bin for any cluster that shares the same initial conditions (but a different initial total cluster mass) of either our tidally-filling or tidally-underfilling models. In the future, for a given set of initial conditions, one needs only simulate clusters over a small range in initial mass to extrapolate the results over the entire initial mass range. Finding the extrapolation of the initial conditions that best intersect with actual Galactic GCs in the $N_{en,i}$-$N_{bin}$ phase space will help to constrain the true initial cluster conditions, as discussed in Section 4.1.

## 4 DISCUSSION

In this section, we discuss the implications of our results for the properties of primordial binaries in Galactic globular

| Bin | Range ($\log_{10}$ ($E_{orb}/E_{avg}$)) | Initial ($\gamma_i$; $\delta_i$) | Filling ($\gamma_i$; $\delta_i$) | Underfilling ($\gamma_i$; $\delta_i$) |
|---|---|---|---|---|
| 1 | -4.0;-3.0 | 0.76; 1.91 | –; – | –; – |
| 2 | -3.0;-2.0 | 1.02; -0.69 | 1.61; -4.73 | 2.39; -9.20 |
| 3 | -2.0;-1.0 | 0.94; -0.30 | 1.20; -1.69 | 1.98; -5.90 |
| 4 | -1.0;0.0 | 0.89; -0.17 | 1.03; -0.69 | 1.26; -1.82 |
| 5 | 0.0;1.0 | 0.83; -0.03 | 0.92; -0.21 | 0.95; -0.30 |
| 6 | 1.0;2.0 | 0.72; 0.25 | 0.87; -0.16 | 0.72; 0.64 |
| 7 | 2.0;3.0 | 0.54; 0.76 | 0.77; -0.03 | 0.19; 2.67 |
| 8 | 3.0;4.0 | 0.20; 1.74 | –; – | –; – |

**Table 2.** Parameters for the lines of best-fit (see Equation 5) for the initial, tidally-filling and tidally-underfilling models. Lines of best-fit are of the form $\log_{10}$ $N_{en,i} = \gamma_i \log_{10} N_{bin} + \delta_i$, where $\gamma_i$ and $\delta_i$ are both constants.

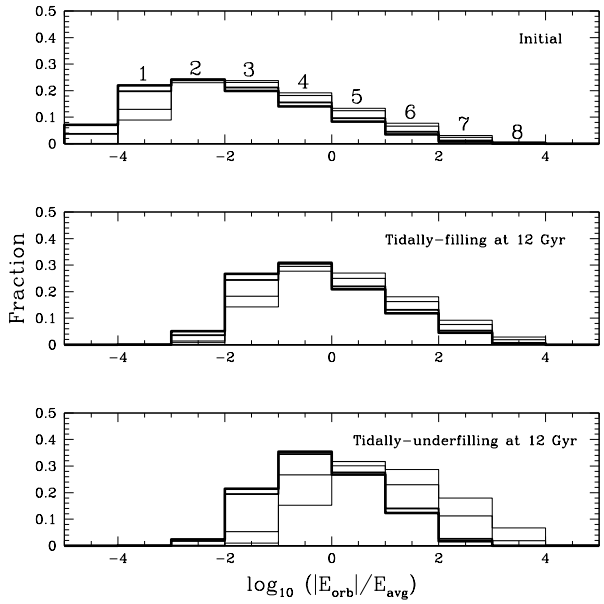


**Figure 4.** The top panel shows the initial (i.e. t = 0) distribution of binary orbital energies for clusters with total initial masses of 5 × $10^4$, $10^5$, 5 × $10^5$ and 8 × $10^5$ $M_\odot$. Note that, if the orbital energies were not normalized by the average kinetic energy in each cluster, the distributions would all be identical at t = 0. Due to our normalization, more massive models have a larger fraction of soft binaries due to the dependence of the hard-soft boundary on the cluster mass. The middle and bottom panels show the orbital energy distributions at 12 Gyr for the tidally-filling and tidally-underfilling models, respectively. The width of the lines forming each histogram correlate with the initial total cluster masses, such that the thickest line had the largest masses. The orbital energies have been normalized by the average single star kinetic energy or $E_{avg} = 0.5 m\sigma^2$, where m is the average single star mass (taken to be 0.35 $M_\odot$ for all models) and $\sigma$ is the root-mean-square velocity. Thus, 0 on the x-axis corresponds to the hard-soft boundary in each cluster. Each histogram bin has been normalized by the total number of binaries (at 12 Gyr) in the corresponding cluster. The numbers shown in the top panel indicate the bins in orbital energy used to generate Figure 5 and shown in Table 2.

clusters, within the framework of the universality hypothesis.

### 4.1 What were the initial binary properties in Galactic globular clusters?

Our results illustrate that the observed present-day binary fractions in Galactic GCs can, to first-order, be reasonably well reproduced assuming universal initial binary properties, specifically a binary fraction near unity, binary orbital parameter distributions resembling those of Kroupa (1995a) and an initial mass-radius relation with high initial densities ($10^4$ - $10^6$ $M_\odot$ $pc^{-3}$). In Leigh et al. (2013a), we demonstrated a similar consistency between the observations and the binary universality hypothesis, but adopting a binary fraction of 10% and an orbital period distribution flat in the logarithm of the binary semi-major axis, while exploring a wide range of initial cluster densities ($10^2$-$10^6$ $M_\odot$ $pc^{-3}$). Importantly, this was for the *central* binary fractions. Thus, as far as the binary *fractions* inside $r_h$ are concerned, the problem of whether or not the primordial binary properties in GCs were universal is degenerate – that is, to first-order, the present-day observations can be reproduced within the universality hypothesis adopting different combinations of the initial binary fraction, binary orbital parameter distributions and mass-radius relations. This was also indirectly

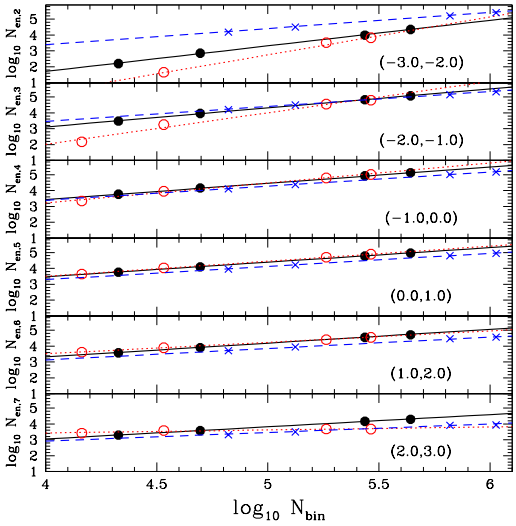


**Figure 5.** Each panel shows the number of binaries $N_{en,i}$ in the corresponding orbital energy bin (indicated in Figure 4) as a function of the total number of binaries $N_{bin}$ in the cluster, for models with total initial masses of $5 \times 10^4$, $10^5$, $5 \times 10^5$ and $8 \times 10^5$ $M_\odot$ (we do not include models with $10^4$ stars initially, since they do not survive to an age of 12 Gyr). The results are shown for the initial distributions at t = 0 (blue crosses), as well as at 12 Gyr for both the tidally-filling (filled circles) and tidally-underfilling (open red circles) models. The range in (normalized) orbital energies corresponding to bin $i$ are indicated in Figure 4 for all six bins shown here, as well as in the lower right of each panel. Lines of best-fit are obtained using Equation 5 and shown for each bin in orbital energy (see Table 2 for the exact fits). The solid black, dotted red and dashed blue lines correspond to the initial, tidally-filling and tidally-underfilling cases, respectively.

demonstrated in Hurley, Aarseth & Shara (2007) using *N*-body models, who showed from a suite of simulations of up to $10^5$ stars that the overall binary fraction remains close to its primordial value (starting with binary fractions on the order of 5%), but increases markedly in the cluster core. Importantly, however, these authors included (mainly) hard binaries only. Thus, in these models, binary destruction in the core is outweighed by mass segregation delivering binaries to the core at a faster rate (combined with binary creation during dynamical interactions).

So how then can we distinguish between degenerate sets of initial conditions? As is illustrated in Figure 1, *the dependence of the present-day binary fraction $f_{b,t}$ outside the half-mass radius $r_h$ on the total cluster mass can break degeneracies that arise using the binary fractions inside $r_h$ alone.* Specifically, assuming an universal initial binary fraction outside $r_h$ along with universal initial orbital parameter distributions, initially tidally-underfilling clusters with high initial densities on the order of $\sim 10^4$-$10^6$ $M_\odot$ $pc^{-3}$ are needed to reproduce the observed anti-correlation between the total cluster masses and the binary fractions in the cluster outskirts. Indeed, lower initial densities yield a *correlation* between $f_{b,t}$ and $M_{clus}$, as illustrated in Figure 1 by the initially tidally-filling models. This is in general consistent with the results of Hurley, Aarseth & Shara (2007) and Fregeau, Ivanova & Rasio (2009), since the mass segregation process operates faster in less massive clusters. In other words, if the overall global binary fraction remains the same while the binary fraction inside $r_h$ increases then the binary fraction outside $r_h$ must decrease (e.g. Fregeau, Ivanova & Rasio 2009), and this process operates the fastest in clusters with the shortest half-mass relaxation times. This leads to a *correlation* between the cluster dynamical age (for which we use the total cluster mass as a proxy in this paper) and the binary fraction outside $r_h$.

Our results are also indicative of an initial mass-radius relation that is less steep than we have adopted here. That is, instead of assuming a constant initial density, the agreement between our models and the observations would improve if we assumed a mean initial density that increases with increasing cluster mass. This is required to obtain a better agreement between our models and the observations for every individual set of models with the same initial conditions but different initial total cluster masses. As seen in Figure 2, the observed dependence of the number of binaries on the total cluster mass is more sub-linear than we obtain in any of our models. Adopting instead an initial-mass radius relation that corresponds to even higher densities in more massive clusters than in our tidally-underfilling models would correct this discrepancy. Thus, assuming an initial mass-radius relation of the form $r_h = \beta M_{clus}^{\alpha}$, our results suggest $\alpha < 1/3$. This is similar to Equation 7 in Marks & Kroupa (2012), who find $\alpha \sim 0.13 \pm 0.04$.

To summarize, assuming global initial binary fractions near unity and the initial binary orbital parameter distributions of Kroupa (1995a) (i.e. most binaries are initially soft), our results are the most consistent with high initial cluster densities of the order $10^4$-$10^6$ $M_\odot$ $pc^{-3}$. We require

the highest initial densities ($\sim 10^6$ $M_\odot$ $pc^{-3}$) to reproduce the observed binary fractions in the most massive Galactic GCs in our sample, and a range at slightly lower initial densities ($\sim 10^4$-$10^5$ $M_\odot$ $pc^{-3}$) to match the observations in the lowest mass GCs in our sample. This suggests an initial mass-density relation corresponding to higher initial densities in more massive clusters (see above). These initial conditions are able to reproduce the observed present-day distribution of binary fractions *both inside and outside the half-mass radius*. Conversely, adopting initial binary fractions near $\sim 10\%$ with a dominant hard binary component combined with comparably high initial densities can reproduce the observed binary fractions *inside* $r_h$ *only*. We emphasize that our results do not necessarily exclude other possible combinations of the initial cluster conditions that might also reproduce the observed data for the Galactic GC population within the framework of the universality hypothesis, nor have we ruled out non-universal initial conditions. For example, our results suggest that the observed binary fractions outside the half-mass radius might be reproducable assuming an universal (global) initial binary fraction of 10% with a dominant hard binary component *if* primordial binary mass segregation is also included in some clusters. With that said, we emphasize that our results, in particular initial cluster densities in the range $10^4$-$10^6$ $M_\odot$ are observed in many massive young star-forming regions, including the ONC, DR21, M17, RCW36, RCW38, NGC1893, etc. (see, for example, Kuhn et al. 2014).

### 4.2 Evolution in energy-space

In this section, we discuss the evolution of the initial binary populations in energy-space as a function of the initial cluster density, both for the initially tidally-filling and tidally-underfilling cases. As we have shown, in those cases where the binary fractions alone are not sufficient to fully remove all degeneracies in the initial conditions (for example, as we have shown, this can be the case inside the half-mass radius), this can be done by also comparing the relative fractions of hard and soft binaries at 12 Gyr.

First, at 12 Gyr, the fraction of hard binaries has increased relative to the initial fraction in all models, as seen in Figure 5. This is the case for both the tidally-filling and tidally-underfilling models, but the effect is more significant for the latter. This is because a higher initial density translates into a larger degree of dynamical processing and hence a larger present-day fraction of hard binaries. Thus, the fraction of hard binaries offers one probe of the initial cluster density. Indeed, as already illustrated via our results for the binary fractions, the fraction of hard binaries in the cluster outskirts (i.e. beyond the half-mass radius) can offer an even more sensitive probe of the initial cluster density. Second, the fraction of hard binaries increases with increasing cluster mass at 12 Gyr, for every set of models sharing the same initial conditions (but different total cluster masses). This is the case for both the tidally-filling and tidally-underfilling models, however the effect is once again more significant for the latter. This is the direct result of our assumed initial mass-density relation. Therefore, the dependence of the hard and soft binary fractions on the present-day total cluster mass (and density) can help to constrain the initial cluster mass-density relation.

It follows from our example application that our extrapolation technique can be used to not only efficiently sample the relevant parameter space of initial conditions, but also to help break any degeneracies (within the universality hypothesis) between the presently observed binary properties and the initial cluster conditions. For example, consider a particular Galactic GC with measured values for both $f_{b,h}$ and $f_{b,t}$. We evolve to 12 Gyr different sets of models having the same initial binary fraction, orbital parameter distributions and mass-density relation (for example, an universal initial binary fraction of 50%, an initial density of $10^3$ $M_\odot$ $pc^{-3}$ and some suitable combination of binary orbital parameter distributions), but different initial total cluster masses. We are not concerned with reproducing the exact present-day total cluster mass in our models at 12 Gyr, but instead generate a range of total cluster masses at 12 Gyr for every set of initial conditions, and then use our extrapolation technique to calculate the distributions of orbital energies at 12 Gyr for the precise total mass corresponding to our cluster of interest. If more than one set of models yields binary fractions that are consistent with the observed binary fractions *both* inside and outside the half-mass radius, this degeneracy can be broken using the relative fractions of hard and soft binaries. That is, the relative fractions of hard and soft binaries, which probe the degree of dynamical processing, should differ. This is quantified by our extrapolation technique. Thus, observational constraints for the relative fractions of hard and soft binaries, if available,[13] can be used to further constrain the initial cluster conditions in those situations where the present-day binary fractions alone cannot fully do the job. Depending on the quality of the data and the degree of degeneracy among the initial conditions, more (or less) binning may be needed to reliably isolate the set of initial conditions that best match the observed data. We note as well that, for a more direct comparison to observed data, our method can just as easily be applied directly to the underlying period, mass ratio and eccentricity distributions instead of the orbital energy distributions. It can also be applied to different spatial subsets of the cluster or different radial bins (e.g. inside and outside the half-mass radius).

Interestingly, in the initially tidally-underfilling case, the fit is poor for our highest bin in orbital energy (i.e. bin 8, which is not shown in Figure 5 or Table 2 since the simple least-squares fits performed for the other orbital energy bins is not appropriate here). This seems to be connected to the earliest stages of cluster evolution, before the clusters have had a chance to expand to fill their tidal radii, since the clusters are initially binary-dominated such that most soft binaries are destroyed during the first few crossing times of the cluster lifetime (Marks, Kroupa & Oh 2011). The models are initially in virial equilibrium, so that they begin to expand on a two-body relaxation timescale (ignoring expansion due to stellar evolution-driven mass loss). It is the most massive clusters that take the longest to expand to fill their tidal radii, since the timescale for two-body relaxation in-

[13] Or perhaps using some proxies for the numbers of hard and soft binaries. For example, the numbers of LMXBs or MSPs can be used as a proxy for the number of hard binaries, and the number of photometric binaries along the MS can be used as a proxy for the total (i.e. hard and soft) number of binaries.

creases with cluster mass. Thus, we postulate that our models deviate from an universal mass-radius relation during the brief period after t = 0 but before all clusters fill their tidal radii. That is, clusters that are not yet tidally-filling retain their binaries in the outskirts so that they continue to be affected by dynamical interactions, whereas tidally-filling clusters lose stars and binaries from their outskirts to the tidal field of the Galaxy. It is this brief high-density state that results in the poor fit seen in the lower panel of Figure 5 for the tidally-underfilling models, since more of the softest binaries are disrupted in the most massive clusters relative to what is seen in Figure 5 for the initially tidally-filling models. This initial phase of differential expansion is avoided altogether in the initially tidally-filling models. We conclude from this that very soft binaries potentially offer the most sensitive probe of the initial cluster conditions.

Importantly, *this phase of differential expansion seen in the tidally-underfilling models contributes to the anti-correlation we see between the binary fractions outside $r_h$ and the total cluster mass.* In the initially tidally-filling models, we find a correlation between $f_{b,t}$ and $M_{clus}$, which is consistent with the results of Hurley, Aarseth & Shara (2007) and Fregeau, Ivanova & Rasio (2009), but inconsistent with the observations (Milone et al. 2012).

### 4.3 Clusters of interest

We emphasize that, while the observed binary fractions for most of the clusters in our sample can be well-reproduced assuming universal initial binary properties, not every cluster fits the mold of binary universality, at least at first glance. In particular, Figure 3 suggests that some clusters may be born with initial binary mass segregation, namely NGC 5466, NGC 5927, NGC 6218 and NGC 7089. This is needed to reproduce the high ratios observed between the binary fractions inside and outside the half-mass radius. NGC 5466 has the lowest mean density inside $r_h$ of all the clusters in our sample, and the difference is greater than an order of magnitude ($\sim$ 20 $M_\odot$ $pc^{-3}$ compared to several 100-1000 $M_\odot$ $pc^{-3}$). This is likely due mainly to the relatively large Galactocentric distance of this cluster (16.3 kpc), which has allowed it to expand considerably over its lifetime (e.g. Webb et al. 2014). However, it does not help to explain the large ratio $f_{b,h}/f_{b,t}$ – unless, perhaps, single stars expand more in the Galactic potential than do binaries, contributing to the appearance of primordial binary mass segregation. NGC 5927 and NGC 6218 have observed Galactocentric distances of 4.6 kpc and 4.5 kpc, respectively. At such small distances from the Galactic centre, mass-loss due to tidal effects from the Galaxy begin to play a very important role. Based on a comparison between the results of MOCCA and NBODY6 at a Galactocentric radius of 4 kpc, MOCCA appears to be under-estimating the rate of mass-loss across the tidal boundary (Madrid, Hurley & Leigh 2014, in preparation). Tides are known to most dramatically affect the cluster outskirts (e.g. Webb et al. 2014) and, if single stars escape at a greater rate than do binaries, this could contribute to lowering the binary fraction outside $r_h$ relative to the value inside $r_h$. More work is needed to properly treat the Galactic potential at small Galactocentric distances, both in MOCCA and in *N*-body models, and hence to address this interesting question.

Another option is that these clusters were born with significant substructure, or in lower mass clusters that eventually merged. In this scenario, the lower initial cluster masses of the sub-clumps translate into shorter two-body relaxation times, and hence shorter mass segregation times for binaries relative to single stars. This could explain the significant concentration of binaries within $r_h$ in these clusters, relative to what we would expect beginning with a single monolothic collapse scenario.

With that said, when the uncertainties on the observed binary fractions are taken into account (Milone et al. 2012), the number of Galactic GCs with binary fractions we are unable to reproduce with our models is very small (with NGC 5927 being the only outlier). It is worth considering whether or not non-members may be contaminating the determination of the binary fractions in these few clusters. Alternatively, multiple stellar populations could be confusing the determination of the binary fractions inside and outside $r_h$, especially if one of these populations has a higher binary fraction or is more centrally concentrated.

### 4.4 Limitations of the Monte Carlo approach

In this section, we briefly highlight several key issues inherent to the Monte Carlo method for simulating globular cluster evolution. Although we do not expect any of these issues to have significantly affected our results, we list them here for completeness.

For our purposes, the most significant issue is MOCCA's treatment of the Galactic tidal field, which is relevant to the rate of escape of single and binary stars across the tidal boundary, and hence the binary fraction in the cluster outskirts. Specifically, MOCCA approximates the Galaxy as a point mass. This means that the rate of stellar evaporation across the tidal boundary is not strictly correct. Regardless, based on previous studies that compared the rate of stellar evaporation in MOCCA to that in *N*-body simulations, which incorporate a more realistic treatment of the Galactic tidal field (e.g. Giersz et al. 2008; Heggie & Giersz 2008), this did not significantly affect our results. Additionally, MOCCA cannot handle time-dependent tidal fields, as is the case for GCs on eccentric orbits (although Sollima & Mastrobuono Battisti 2014 recently proposed a method to address this issue within the Monte Carlo approach). Thus, our results are based on simulations of GCs placed on purely circular orbits, since MOCCA *can* treat a static tidal field with comparable accuracy to currently available *N*-body codes (Fukushige & Heggie 2000).

There are two primary sources of stochasticity in the MC method. The first relates to the determination of the position of an object along a given orbit. At each time-step, the position is determined according to the probability of finding an object in a particular location along its orbit. At each subsequent time-step, a new position is determined, and this can differ substantially from the previous position. This leads to stochastic changes in the gravitational potential between time-steps. The second source of stochasticity pertains to the outcomes of dynamical encounters involving binaries. The initial conditions going into the dynamical encounters (whose outcomes are calculated using the FEWBODY code) are also mildly stochastic, due to the aforementioned stochastic changes to the positions of objects be-

tween time-steps. This translates into some stochasticity in the outcomes of the interactions, since these depend sensitively on the initial interaction conditions.

We do not expect either of these sources of stochasticity to have significantly affected our results. We tested this by re-running the models with the same initial conditions, but using different random seed values for the random number generators. Our results always yield the same final cluster parameters (half-mass radius, density, mass, etc.) to within typically a few percent. The only exception to this is the core radius, which fluctuates significantly (by as much as a factor of a few) from time-step to time-step. Importantly, however, this is the case not only for the Monte Carlo approach, but also for $N$-body models for star cluster evolution (e.g. Webb et al. 2014).

Other limitations of the Monte Carlo method include deviations from spherical symmetry including rotation (however Vasiliev recently proposed a method to circumvent this issue using the Monte Carlo method; private communication), sudden changes in the gravitational potential (e.g. violent relaxation or sudden gas removal) and hierarchical multiples (e.g. encounters involving triple stars, quadruples, etc.). Most of these issues are currently being investigated, and should be included in the MOCCA code in the near future. The Monte Carlo method also requires that the local time-step is always a fraction of the local relaxation time, which must always be longer than the local dynamical time of the system. This condition is always satisfied in our models, particularly during the first few Myr of cluster evolution when most (soft) primordial binaries are disrupted due to dynamical encounters.

## 5 SUMMARY

In this paper, we consider the origins of the binary properties observed in Galactic globular clusters. To this end, we present the results of a suite of Monte Carlo models for GC evolution performed using the MOCCA code (Giersz et al. 2013), which we compare to the observed present-day binary fractions of Milone et al. (2012).

In Paper I, we showed that the observed distribution of present-day *central* binary fractions can be reproduced assuming an universal initial binary fraction of 10%, a period distribution flat in the logarithm of the binary orbital semi-major axis and moderate initial densities close to the present-day values observed in Galactic GCs ($\sim 10^2$-$10^3$ $M_\odot$ $pc^{-3}$). In this paper, we consider instead an universal initial binary fraction near unity, the binary orbital parameter distributions of Kroupa (1995a) (i.e. with a significant soft binary component) and high initial densities ($10^4$-$10^6$ $M_\odot$ $pc^{-3}$). Our results suggest that, to first-order, the present-day binary fractions inside the half-mass radius are degenerate. That is, they can be reproduced assuming either initially low binary fractions with a dominant hard component and moderate densities, or initially high binary fractions with a dominant soft component and high densities. We show that the observed present-day binary fractions *outside* the half-mass radius can break this degeneracy. In this regard, our results are the most consistent with high initial binary fractions and high initial densities, since these conditions are needed to reproduce the observed anti-correlation between the total cluster mass and the observed binary fractions outside $r_h$. To reproduce the slope of this anti-correlation, our results favour an initial mass-density relation $r_h \propto M_{clus}^{\alpha}$ with $\alpha < 1/3$. This corresponds to initially more massive clusters having higher initial densities, in rough agreement with the results of Paper I of this series (Leigh et al. 2013a). Additionally, the observed present-day mean densities inside $r_h$ are typically in the range $\sim 10^2$-$10^4$ $M_\odot$ $pc^{-3}$ for Galactic GCs (Harris 1996, 2010 update), which agree better with our initially tidally-underfilling models.

Thus, we require high initial densities ($\sim$ $10^4$-$10^6$ $M_\odot$) with initially tidally-underfilling clusters to reproduce the *observed* anti-correlation between binary fraction and cluster mass outside $r_h$, in conjunction with present-day densities that agree with the observed range in Galactic GCs. Importantly, such high densities have actually been observed in young massive star-forming regions (e.g. Hillenbrand & Hartmann 1998; Kuhn et al. 2014).

We further apply the extrapolation technique first introduced in Leigh et al. (2012) to the initial and final binary orbital energy distributions, in order to quantify the degree of dynamical processing as a function of the assumed initial conditions. We illustrate that our method can be used to constrain both the initial cluster density as well as the initial mass-density relation, if/when more sophisticated observations become available for the underlying present-day binary orbital parameter distributions in GCs. We have only applied our technique using two different initial mass-density relations (i.e. the tidally-filling and tidally-underfilling sets of models) and a single universal set of binary fractions and orbital parameter distributions, using these as a "proof-of-concept" for our method and to highlight some of the effects of the assumed initial cluster density. In principle, however, our method can be applied to *any* choice of initial mass-density relation combined with *any* choice of initial binary fractions and orbital parameter distributions (assuming they are either universal or show a clear and direct dependence on the initial mass-density relation). This offers the potential for future studies to generate an extensive set of simulated old ($\sim$ 12 Gyr) GCs spanning three decades in present-day total cluster mass with minimal computational expense.

As an overall conclusion, the results of this work are consistent with primordial GCs having formed with universal stellar populations in terms of both the initial mass function and the initial binary properties for stars less massive than $\sim$ 1 $M_\odot$. For at least this stellar mass range, there is no evidence to suggest that the initial binary populations were significantly different a Hubble time ago in young massive clusters compared to what is observed today in nearby, young and sparse star-forming regions in the Milky Way disk.

## ACKNOWLEDGMENTS

This work was partly supported by the Polish Ministry of Science and Higher Education, and by the National Science Centre through the grants DEC-2012/07/B/ST9/04412 and DEC-2011/01/N/ST9/06000. NL, JW, AS and COH all gratefully acknowledge the support of NSERC. MM was partly supported through DFG grant KR 1635/40-1. COH

also acknowledges the support of an Alberta Ingenuity New Faculty Award.

## REFERENCES


Bastian N., Strader J. 2014, MNRAS, accepted

Baumgardt H. 2001, MNRAS, 325, 1323

Binney J., Tremaine S., 1987, Galactic Dynamics (Princeton: Princeton University Press)

Cohn H. N., Lugger P. M., Couch S. M., Anderson J., Cool A. M., van den Berg M., Bogdanov S., Heinke C. O., Grindlay J. E. 2010, ApJ, 722, 20

Conroy C., Spergel D. N. 2011, ApJ, 726, 36

Conroy C. 2012, ApJ, 758, 21

De Angeli F. Piotto G., Cassisi S., Busso G., Recio-Blanco A., Salaris M., Aparicio A., Rosenberg A. 2005, AJ, 130, 116

Duchêne G., Bouvier J., Simon T. 1999, A&A, 343, 831

Fellhauer M., Kroupa P., Evans N. W. 2006, MNRAS, 372, 338

Ferraro F. R., Lanzoni B., Dalessandro E., Beccari G., Pasquato M., Miocchi P., Rood R. T., Sigurdsson S., Sills A., Vesperini E., Mapelli M., Contreras R., Sanna N., Mucciarelli A. 2012, Nature, 492, 393

Fregeau J. M., Cheung P., Portegies Zwart S. F., Rasio F. A. 2004, MNRAS, 352, 1

Fregeau J. M., Ivanova N., Rasio F. A. 2009, ApJ, 707, 1533

Fukushige T., Heggie D. C. 2000, MNRAS, 318, 753

Geller A. M., de Grijs R., Li C., Hurley J. R. 2013, ApJ, 779, 30

Giersz M., Heggie D. C., Hurley J. R. 2008, MNRAS, 388, 429

Giersz M., Heggie D. C., Hurley J. R., Hypki A. 2013, MNRAS, 431, 2148

Gratton R. G., Bonifacio P., Bragaglia A., Carretta E., Castellani V., Centurion M., Chieffi A., Claudi R., Clementini G., D'Antona F., Desidera S., Francois P., Grundahl F., Lucatello S., Molaro P., Pasquini L., Sneden C., Spite F., Straniero O. 2001, A&A, 369, 87

Gratton R., Carretta E., Bragaglia A. 2012, Astronomy & Astrophysics Review, in press (arXiv:1201.6526)

Hansen B. M. S., Kalirai J. S., Anderson J., Dotter A., Richer H. B., Rich R. M., Shara M. M., Fahlman G. G., Hurley J. R., King I. R., Reitzel D., Stetson P. B. 2013, Nature, 500, 51

Harris, W. E. 1996, AJ, 112, 1487 (2010 update)

Heggie D. C. 1975, MNRAS, 173, 729

Heggie D. C., Giersz M. 2008, MNRAS, 389, 1858

Henon M. 1971, Ap&SS, 13, 284

Hillenbrand L. A., Hartmann L. W. 1998, ApJ, 492, 540

Hills J. G. 1975, AJ, 80, 809

Hurley J. R., Pols O. R., Tout C. A. 2000, MNRAS, 315, 543

Hurley J. R., Pols O. R., Tout C. A. 2002, MNRAS, 329, 897

Hurley J. R., Aarseth S. J., Shara M. M. 2007, ApJ, 665, 707

Hut P., Murphy B. W., Verbunt F. 1991, A&A, 241, 137

Hypki A., Giersz M. 2013, MNRAS, 429, 1221

Kroupa P., Gilmore G., Tout C. A. 1991, MNRAS, 251, 293

Kroupa P., Tout C. A., Gilmore G. 1993, MNRAS, 262, 545

Kroupa P. 1995, MNRAS, 277, 1491 (Kroupa 1995a)

Kroupa P. 1995, MNRAS, 277, 1522 (Kroupa 1995b)

Kroupa P. 2008, Cambridge *N*-body Lectures, Lecture Notes in Physics, 760. Springer-Verlag, Berlin, p. 181

Kroupa P., Weidner C., Pflamm-Altenburg J., Thies I., Dabringhausen J., Marks M., Maschberger T. 2013, Planets, Stars and Stellar Systems Vol. 5, ed. Oswalt T. D. & Gilmore G. (Springer Science & Business Media Dordrecht: Dordrecht), 115-242

Kruijssen J. M. D., Lützgendorf N. 2013, MNRAS Letters, accepted (arXiv:1306.0561)

Kuhn M. A., Feigelson E. D., Getman K. V., Baddeley A. J., Broos P. S., Sills A., Bate M. R., Povich M. S., Luhman K. L., Busk H. A., Naylor T., King R. R. 2014, ApJ, 787, 107

Leigh N. W. C., Sills A. 2011, MNRAS, 410, 2370

Leigh N. W., Umbreit S., Sills A., Knigge C., De Marchi G., Glebbeek E., Sarajedini A. 2012, MNRAS, 422, 1592

Leigh N. W., Knigge C., Sills A., Perets H. B., Sarajedini A., Glebbeek E. 2013, MNRAS, 428, 897

Leigh N. W., Giersz M., Webb J. J., Hypki A., De Marchi G., Kroupa P., Sills A. 2013, MNRAS, 436, 3399

Marin-Franch A., Aparicio A., Piotto G., Rosenberg A., Chaboyer B., Sarajedini A., Siegel M., Anderson J., Bedin L. R., Dotter A., Hempel M., King I., Majewski S., Milone A. P., Paust N., Reid I. N. 2009, ApJ, 694, 1498

Marks M., Kroupa P. 2010, MNRAS, 406, 2000

Marks M., Kroupa P., Oh S. 2011, MNRAS, 417, 1684

Marks M., Kroupa P. 2012, A&A, 543, 8

Marks M., Leigh N., Giersz M., Pfalzner S., Pflamm-Altenburg J., Oh S. 2014, MNRAS, 441, 3503

Milone A. P., Piotto G., Bedin L. R., Aparicio A., Anderson J., Sarajedini A., Marino A. F., Moretti A., Davies M. B., Chaboyer B., Dotter A., Hempel M., Marin-Franch A., Majewski S., Paust N. E. Q., Reid I. N., Rosenberg A., Siegel M. 2012, A&A, 540, 16

Naoz S., Fabrycky D. C. 2014, ApJ, submitted (arXiv:1405.5223)

Osborn W. 1971, Observatory, 91, 223

Parker R. J., Goodwin S. P., Kroupa P., Kouwenhoven M. B. N. 2009, MNRAS, 397, 1577

Perets H. B., Fabrycky D. C. 2009, ApJ, 697, 1048

Pflamm-Altenburg J., Kroupa P. 2007, MNRAS, 375, 855

Pflamm-Altenburg J., Kroupa P. 2009, MNRAS, 397, 488

Piotto G., Bedin L. R., Anderson J., King I. R., Cassisi S., Milone A. P., Villanova S., Pietrin- ferni A., Renzini A. 2007, ApJ, 661, L53

Pooley D., Hut P. 2006, ApJL, 646, L143

Salaris M., Weiss A., 2002, A&A, 388, 492

Sigurdsson S., Phinney E. S. 1993, ApJ, 415, 631

Sippel A. C., Hurley J. R. 2013, MNRAS, 430, 30

Sollima A., Beccari G., Ferraro F. R., Fusi Pecci F., Sarajedini A. 2007, MNRAS, 380, 781

Sollima A. 2008, MNRAS, 388, 307

Sollima A., Mastrobuono Battisti A. 2014, MNRAS, 443, 3513

Verbunt F., Lewin W. H. G., van Paradijs J. 1989, MNRAS, 241, 51

Vishniac E. T. 1978, ApJ, 223, 986
Webb J.J., Harris W. E., Sills A., Hurley J. R. 2013, ApJ, 764, 124
Webb J.J., Leigh N., Sills A., Harris W. E., Hurley J. R. 2014, MNRAS, 442, 1569

This paper has been typeset from a TEX/ LATEX file prepared by the author.